JOURNAL OF AIRCRAFT
Vol. 45, No. 6, November–December 2008

Aircraft Icing in Glaciated and Mixed Phase Clouds

John Hallett*
Desert Research Institute, Reno, Nevada 89512
and
George A. Isaac†
Environment Canada, Toronto, Ontario M3H 5T4, Canada

DOI: 10.2514/1.37596

Aircraft are typically certified for flight into clouds containing entirely supercooled liquid particles. Nevertheless, mixed-phase clouds containing both supercooled water and ice particles occur not infrequently under similar atmospheric conditions at temperatures down to at least −30°C and, on occasion, to −40°C and are not included in the specification. Characterization of such clouds has proved a challenge to our understanding and measurement capability. As was recognized a decade ago, the role of such clouds in aircraft icing incidents is unclear and merits attention. Further, the definition of mixed-phase clouds depends on aircraft-borne instruments, their ability to differentiate between ice and water separately, and their time response with respect to the actual spatial distribution of ice and water with respect to the aircraft track. Such mixed phase clouds vary from an intimate mix of cirrus ice falling into a supercooled cloud layer to a consideration of a cumulonimbus system of a supercooled cloud updraft adjacent to an ice downdraft, but many kilometers distant. The scale of the mix must therefore be considered in terms of physical processes of updraft and downdraft. The impact on aircraft performance is highly dependent on the flight time in regions of any particular mix. Individual particles are investigated following impact on a heated 2-cm-diam sapphire optical flat (the cloudscope), mounted normal to the airflow and having a central stagnation point, and video recorded from behind. Impacting particles diverge, melt, and/or evaporate, the rate of area change being a measure of particle density. The relative mix of particle phase, size, shape, and concentration provides insight on accretion scenarios for possible aircraft structural or engine performance degradation.

I. Introduction

AIRCRAFT are typically certified for flight into icing conditions that contain only supercooled liquid particles, according to FAR 25 Appendix C [1]. However, as shown by Cober and Isaac [2], mixed-phase clouds occur quite frequently, accounting for approximately 40–50% of the in-cloud encounters at temperatures between 0 and −30°C.

Following the Avions de Transport Regional crash in Roselawn, Indiana in 1994 and the Embraer 120RT Brasilia crash in Monroe, Michigan in 1997, the National Transportation Safety Board requested the FAA to "expand the Part 25 Appendix C icing certification envelope to include freezing drizzle/freezing rain and mixed water/ice crystal conditions as necessary" [3,4]. Partly as a result of this recommendation, the FAA hosted a specialists meeting on mixed-phase and glaciated conditions [5]. It was clear from this meeting that mixed-phase and glaciated conditions were not generally recognized as being dangerous or even necessary to consider as a hazard beyond that posed by the liquid fraction of the clouds encountered by the aircraft. This paper attempts to open debate and characterize the icing potential due to ice crystals in mixed-phase and glaciated clouds.

The concept of mixed-phase clouds requires definition. One approach, seen in Cober et al. [6] and Korolev et al. [7], averages liquid and ice-water content over selected intervals of 30 s (3 km) or 1 s (100 m), respectively, and examines the fraction of water/ice with extremes of all water or all ice. The measurements may be refined to shorter distances with higher-resolution instruments [8,9]. A consideration of different physical processes suggests that intimate ice–water mixes may occur following seeding of a lower-level supercooled cloud (stratus) from a widespread cloud aloft (e.g., cirrus) by initiation of ice by uniformly distributed nuclei, by lifting of ice-containing air in a convective element, or a stationary or progressive gravity wave. In contrast, regions of supercooled water and ice may occur in clouds with embedded convection, with all water in the upshear vertical motion and all ice present in the downshear descending air. The scale of mixed water–ice regions will depend on the scale of the convection, ranging from 10 m to l0 km [10] or even longer for mountain-induced waves.

Mixed phase is necessarily an arbitrary yet definable quantity. Water and ice may be intimately mixed, as in a melting snowflake, or less so, as in a cloud with separated water and ice particles spatially dispersed at random. A mix is also produced in varying proportion by a cirrus layer sprinkling into a supercooled cloud layer below. We may choose to define a region of space as mixed phase should it be smaller than the measurement resolution, yet still have regions of all water and regions of all ice with definitive interface regions, measurable should the resolution be increased. Thus, a deep cumulonimbus cloud may consist of a supercooled water updraft together with an anvil and an ice downdraft; the cloud as a whole may be considered as mixed phase, although high-resolution top to bottom and upshear to downshear considered separately will show distinct regions of ice or water cloud. In particular, the interface regions between all water and all ice examined at a sufficiently high resolution must necessarily reveal the presence of mixed-phase clouds, the sharpness of the interface now being subject to the statistics of the spatial distribution of particles subject to local mixing. The icing potential of any mixed-phase volume is therefore definable for a given flight trajectory but requires a scale specification to be complete.

Sequential events under changing conditions may lead to buildup of complex ice shapes on aerofoil surfaces and seriously compromise the flight behavior of the aircraft. De-icing strategies depend on a knowledge of these processes, with the detail design for the removal

Presented as Paper 0677 at the 40th AIAA Aerospace Sciences Meeting and Exhibit, Reno, Nevada, 14–17 January 2002; received 17 March 2008; revision received 12 June 2008; accepted for publication 14 June 2008.

*Research Professor, Division of Atmospheric Sciences, 2215 Raggio Parkway.
†Senior Scientist, Cloud Physics and Severe Weather Research Section, 4905 Dufferin Street.

of accreted ice by heating or otherwise depending critically on the assumptions of whether the ice needs to be completely melted and evaporated or whether melt at the ice/aircraft surface interface will allow the ice to be removed to the ambient airstream through surface detachment alone. The detail of the interaction of particles of different phase, size, density, and shape with the aircraft surface is complicated in itself and depends further on the impact velocity and angle, the surface and particle temperature, and also on the changing surface and geometry of the accreting surface. Further, the atmosphere is a highly variable environment with major changes in particle type, size, and concentration within cloud and precipitating systems, with discontinuities over distances less than 1 m or 0.01 s of flight time [11]. The studies reported herein were designed to provide insight into the particle impact and ice buildup process by direct video viewing during flight through a variety of icing conditions during the Alliance Icing Research Study (AIRS I), described by Isaac et al. [12], and during AIRS II, conducted during the winter of 2003/2004 [13]. Data were also taken from the penetration of the outflow of hurricane Earl, Convection and Moisture Experiment 1998, off Florida and during the Kwajelein Experiment in mid-Pacific convection. This was accomplished by use of the cloudscope, which video records (at 1/30–1/90 s, as necessary) the particle–surface interaction events and provides quantitative analysis of the impaction, the accretion, and the phase change process.

II. Instrumentation

Measurement of the properties of ice particles in the atmosphere, specifically density and shape (habit), is important in determining their role in modifying radiation flux and also in estimating the ice–water content from imaging probes such as Particle Measurement Systems 2-D cloud and precipitation and Stratton Park Engineering Company's Cloud Particle Imager [14,15]. A Desert Research Institute cloudscope was designed to measure cloud properties by collecting, melting, and evaporating cloud particles [16–18] and has provided insight into the collection and evolution of particles important for aircraft icing. The principle of operation is to collect the particles on a forward-facing optical flat maintained at approximately the total temperature. Particles are video imaged from behind and evaporate or melt under known conditions to give a measure of their initial shape, together with their density and the density distribution within the particle [19]. The temperature may be raised to give more rapid evaporation for a higher collection rate and is measured directly by a sensor at the edge of the window. Figures 1 and 2 show instruments having a field of view of $\frac{1}{2}$ mm and 1–2 cm. The stagnation point is approximately in the center of the field of view, so that impactions and particle behavior away from this location may readily be observed. It is also possible to examine the impaction of particles from the side using a suitably located and de-iced prism (Fig. 3). The advantage of this system for icing studies is that the surface may be heated above 0°C to simulate particle impaction and melt in an actively heated surface. Particle behavior on impaction may also be investigated by an older instrument, the Formvar replicator [20,21], whereby particles of size greater than a few micrometers are collected in a thin layer of Formvar solution on a 16 mm film moving at 1–48 cm/s and dried to leave a cast of the particles for future microscopic analysis. The shatter and collection of resulting particles is easily recorded by this technique, although there may be some cushioning of the impact by the solution. Both instruments were mounted in standard pods on the wing tips of the Canadian Convair, protruding a meter or so into the airstream, and in the wing tip pods of the NASA DC8. The pods are de-iced around the collecting regions, a process that is, in general, sufficient to prevent any significant buildup. The angle of attack at the sensing region tip is necessarily subject to some uncertainty should the aircraft be in maneuver or turbulence, leading to a changing location of the stagnation point.

The cloudscope enables the local stagnation point to be monitored within limits by applying a transitory melting pulse to the window and observing the trajectory of the drops from the melted ice on the heated surface. The sapphire window can be operated at temperatures up to about +30°C and even at air temperatures down to −40°C, and the behavior of impacting ice particles can be examined.

A. Airflow of a Rapidly Approaching Particle to an Aircraft Surface

For any particle approaching a surface, such as a drop or ice crystal impacting on an aircraft wing, the intervening air is forced out and the

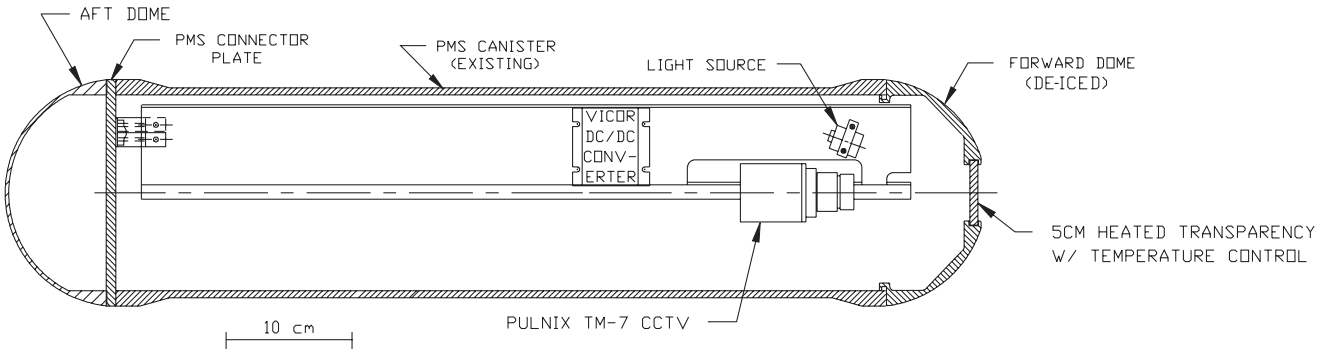

Fig. 1 Large format cloudscope with 5-cm-diam sapphire window with 4 cm exposed and a sample volume of 5–50 l/s

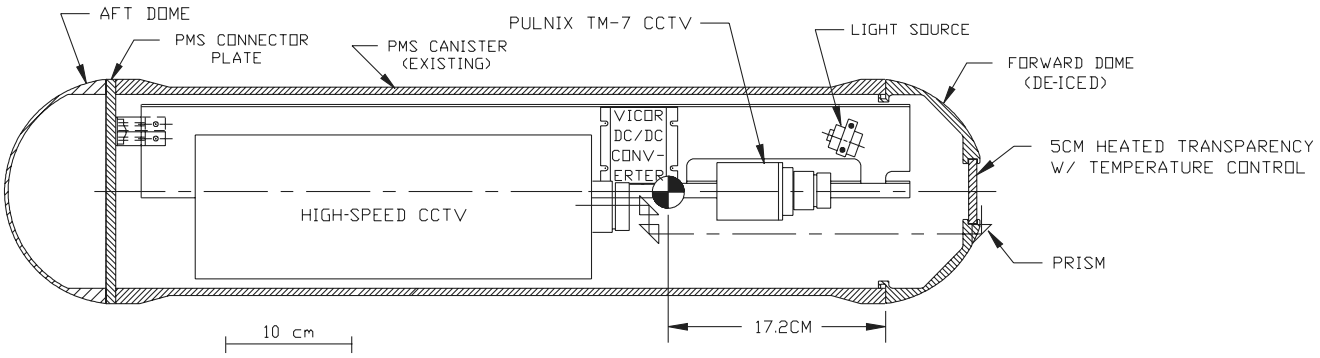

Fig. 2 Large format cloudscope with a high-speed side-looking closed-circuit television.

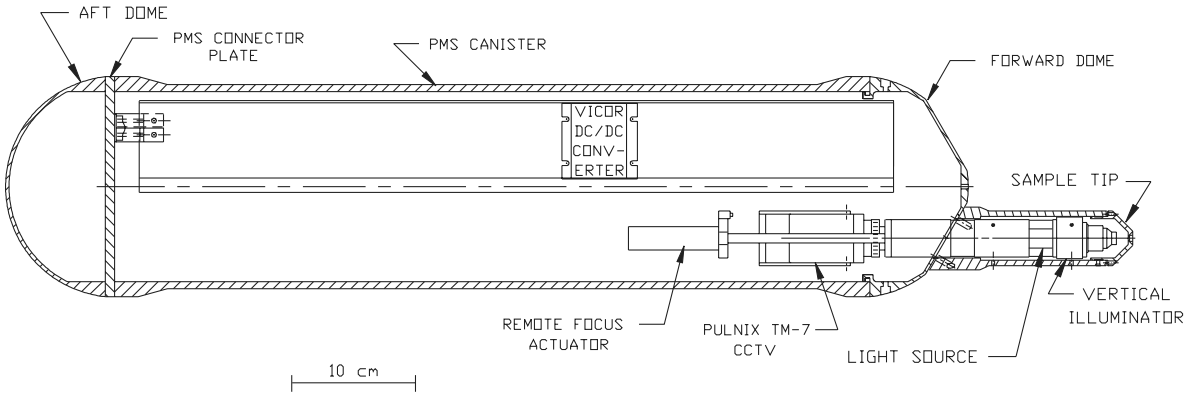

Fig. 3 Small format cloudscope with 0.3 × 0.3 cm sapphire window field of view and a sample volume of 25–50 $cm^3 s^{-1}$. Instruments are readily exchanged in a standard aircraft-mounting pod.

impacting particle is slowed and possibly deformed and/or shattered. The geometry of the flow is complex; in the case of a drop, an air cavity forms due to pressure buildup as the drop spreads sideways, with air escaping at high velocity near the periphery [22]. In the case of a rigid ice particle, particularly at a higher density of >0.4 g/cm^3, and for the normal impact of a facet, the particle deforms much less and air exit velocity is much greater, increasing to high values as a lateral disklike jet of air. This jet appears capable of removing ice particles a diameter or more distant and thus eroding previously accreted ice particles, an effect readily demonstrated in cloudscope images. A drop approaching a flat surface first flattens and then spreads laterally as a disk with trapped air, sometimes between water and surface, moving outward at a velocity proportional to impact velocity V, radius r, and thickness x of the air layer. Continuity considerations suggest a relationship of the outward velocity of the form rV/x and a large outward velocity of greater than 100 m/s at the edge of the expansion for an air thickness of tens of μm, possibly approaching sonic speeds, but limited by viscous effects. An ice crystal approach will behave similarly, without deformation, but with breakup at sufficient impact velocity. The efficacy of such a process is clearly demonstrated by observation of the interaction between two drops accreting nearly simultaneously at several drop diameters of separation, which produces lateral water jets in opposing directions parallel to the impaction surface at 90 deg to the direction of the approaching water disks resulting from the initial impact of each drop separately. The outward jet velocities are well in excess by a factor of 10 of the particle impact velocity and, on occasion, may be mistaken for an ice crystal.

B. Observations

The collection of individual ice particles at and near the stagnation point is clearly shown in Figs. 4–7. These particles, with sizes of several hundred μm, evaporate over a few seconds, with an area–time plot for each particle giving a measure of its density. Such behavior may occur for rimed particles and also particles having subsequently grown from the vapor from a more solid interior (Fig. 5). Measured densities range over 0.05 to solid ice, 0.9 g/cm^3, depending on conditions [23]. In a given situation, the variance may lie at $+/-0.2$ g/cm^3 of a mean value (Fig. 8). Some particles have a linear area–time plot showing a constant density over the radius of the particle; others may show one or occasionally more discontinuities in slope, indicating sudden changes in density, usually with a fluffy outside and a more solid interior. Such particles may result from vapor growth on a previously frozen drop [24].

Individual crystals as columns or plates may fracture on impact for a size greater than about 200 μm, but often fail to separate significantly. Figures 9–11 illustrate crystals collected under these circumstances. The behavior at an angled impact should be quite different and is being investigated by an optical and impact system, tilted with respect to the flow.

A sideways view gives a different perspective of the accretion process and enables the shape of the accreted particle to be examined. For example, Fig. 12 shows a sequence of images as the cloudscope window is cooled. Initially, the images give the appearance of liquid drops hitting the window. But as the window is cooled to below freezing, it becomes clear that the particles were actually ice particles, which eventually coat the window with a layer of ice. Figure 13 shows the impact of incoming particles on or near existing particles undergoing evaporation. A particle arriving within a diameter or two of an existing particle may lead to its disappearance within the time between video images, 1/30 s. The impact gives rise to an outward-moving cylindrical disk of air, becoming shallower and moving faster as the ice particle approaches the surface as described earlier. This outward-moving radial jet forces the nearby particle to take off. With an increased accretion rate of particles at high concentration, the layer of ice near the stagnation point grows until reaching some sort of equilibrium between impaction, accretion, and erosion, from 0.3 to up to 5 mm in thickness (Fig. 13). The video shows particles entering and leaving over the time of the frame interval (0.1 s). It is of interest that, during flight through known all-ice conditions, the presence of such icing can often be detected visually as a white strip along the stagnation lines of unheated leading edges. Once in clear air and for slow ice accretion rates, such regions slowly sublimate as they are at the total air temperature and the ice is subsaturated with respect to its immediate environment.

With the temperature of the cloudscope collecting surface raised from a few degrees to $+10$ deg above 0°C, particles <100 μm can be seen to melt over a few frames on collection. Above $+10$°C, such particles melt in a period of less than a frame of the video record and appear mostly as liquid droplets with occasional flashes of light from favorably oriented facets of impacting ice particles. In either case, the particles can be seen spreading outward from the stagnation point with the local airflow at a velocity of a few centimeters per second or less (Figs. 14 and 15). Larger ice particles, >100 μm, persist for correspondingly longer times depending on their density and are carried to the edge of the field of view (Fig. 16). The presence of supercooled drops is inferred as they accrete and spread as disks failing to show the presence of any facets.

III. Discussion

A. General Energy Considerations

Particle impaction on any aircraft surface during flight is related to the extent the particle follows or crosses the streamlines around the surface, which in turn depends on particle inertia and drag. The former is related to the particle mass and its density distribution, the latter to its shape and orientation to the local flow. Aerosol and small cloud droplets are carried away in the flow; larger hailstones impact directly with little influence on their fall motion. Intermediate-sized particles impact with a reduced velocity preferentially at leading edges, undergoing some acceleration to approach aircraft velocity before impact. Here we are concerned with the nature of this impact with lower relative velocity and whether the particles break, bounce,

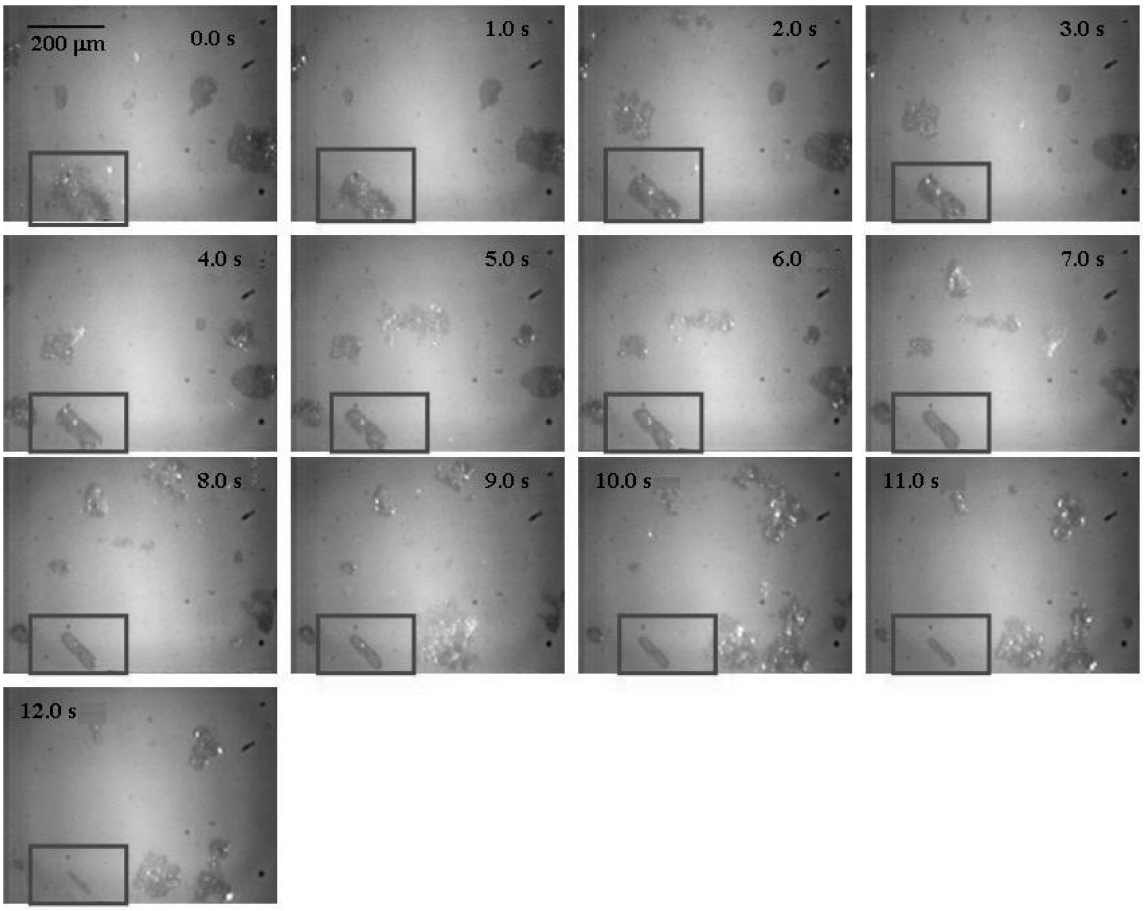

Fig. 4 Cloudscope images of individual evaporating ice particles. A rimed column, as it sublimated the rime, is removed, revealing the column.

crumble, or adhere to or wet the surface. As a guide to this interaction, it is useful to consider a modified Weber number (L) [25], the ratio of the particle impact kinetic energy to its surface energy:

$$L = \text{kinetic energy/surface energy} \tag{1}$$

For a spherical water drop,

$$L = \tfrac{1}{2} m \, \mathrm{V}^2 / A\sigma \tag{2}$$

where m is the drop mass, A is the drop surface area of πD^2, V is the drop impact velocity normal to the surface, D is the drop diameter, and σ is the drop surface energy. For a sufficient approximation at 0°C,

$$L = DV^2/1000 \tag{3}$$

For an ice crystal, the particle mass is to be calculated from the knowledge of its shape and density or density distribution if asymmetrical. Should particles splash or break up, the incoming kinetic energy is to be appropriately reduced by the exiting kinetic energy. Laboratory studies show that L lies between 7–10 for drop breakup and splash for impacting on a rough surface. Figure 17 suggests that both drizzle and raindrops splash on accretion at aircraft speeds when $L > 10$, whereas cloud droplets may be sufficiently decelerated to accrete without breakup. For an ice particle things are much more complex, and shatter into a few particles is demonstrated to occur for particles collected in a Formvar-solution-coated film for ice plates greater than about 200–300 μm (Fig. 9). A plate some 500 μm across has sufficient energy when impacted at aircraft speed to shatter into more than 1000 pieces (Fig. 10) [9,21]. Similar criteria apply to three-dimensional particles radiating from a single nucleating point as spatial columns or plates (Fig. 11). Graupel (soft hail) particles and snowflakes tend to crunch on impact, yet, as is the case for plates, retain their coherency up to a size of a few millimeters. Limitations of energy availability provide better insight into the relevant physical processes; the minimum amount of energy required to break a sphere or disk in half is equivalent, with sufficient accuracy, to a velocity U:

$$U = 4\sqrt{\frac{\sigma}{\pi D \rho}} \tag{4}$$

where σ is the appropriate surface energy, ρ is the particle density, and D is the particle diameter. Taking $\sigma = 0.12$ J/m^2 and $\rho = 920$ kg/m^3, the velocity to break in half for $D = 10$, 100, and 1000 μm is 8.15, 2.58, 0.82 m/s, respectively. This is well below aircraft impact velocities, and so significant breakup is highly likely.

Should particles skid or bounce, a significant amount of energy may be lost and be unavailable for breakup. This process has important implications for de-icing power requirements, as such bouncing particles would not enter the requirements of energy for complete evaporation or melt as computed by an accretion rate from a measurement of ice–water content. Because the current thinking is that *all* such ice particles bounce (aircraft do not usually ice up on penetration of all-ice clouds), it is important to establish the conditions for these different scenarios. A further possibility lies in the *erosion* of accreted ice by incoming ice particles, as seen in Figs. 7 and 13, giving the appearance of particle bounce. More important is the likelihood of a small amount of supercooled cloud acting as a "glue" for the accretion of ice particles when present in small (10%) and difficult-to-measure concentrations [8]. All accreted particles, liquid and solid, from a few millimeters down to a few microns in size collected at or near the stagnation point were measured. Figure 16 shows melting beginning near the stagnation point and spreading outward as the window is heated. Incoming ice particles appear, begin melting in the liquid layer, and are carried to the expanding ice–water interface in the divergent flow to the edge of the window.

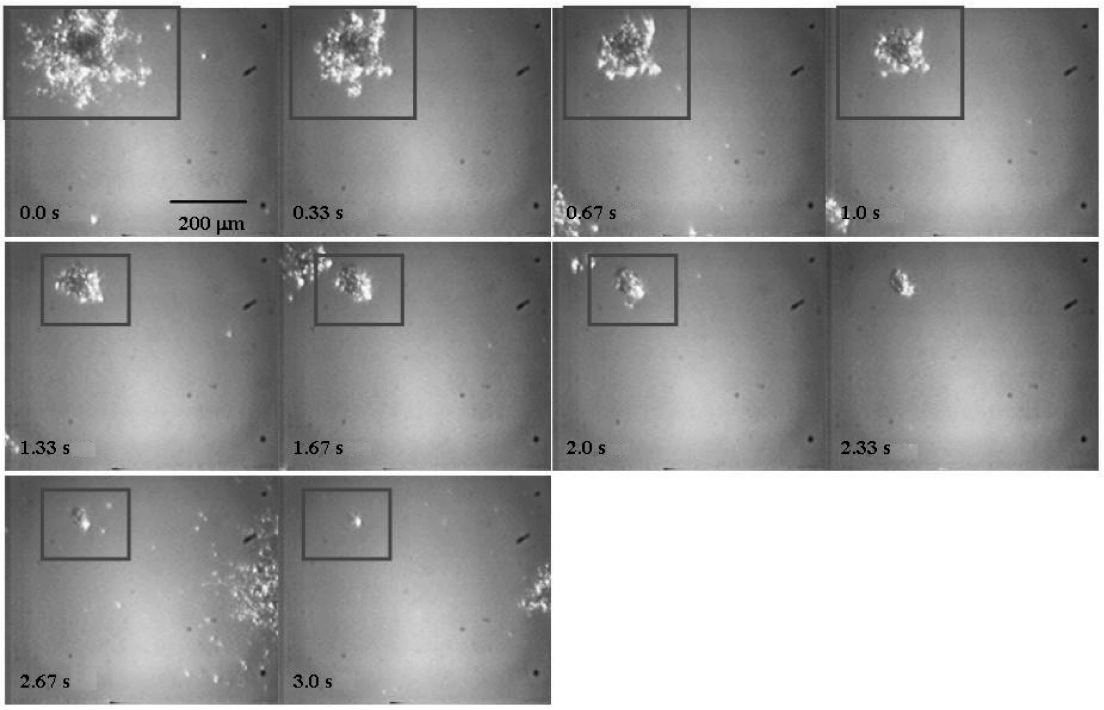

a)

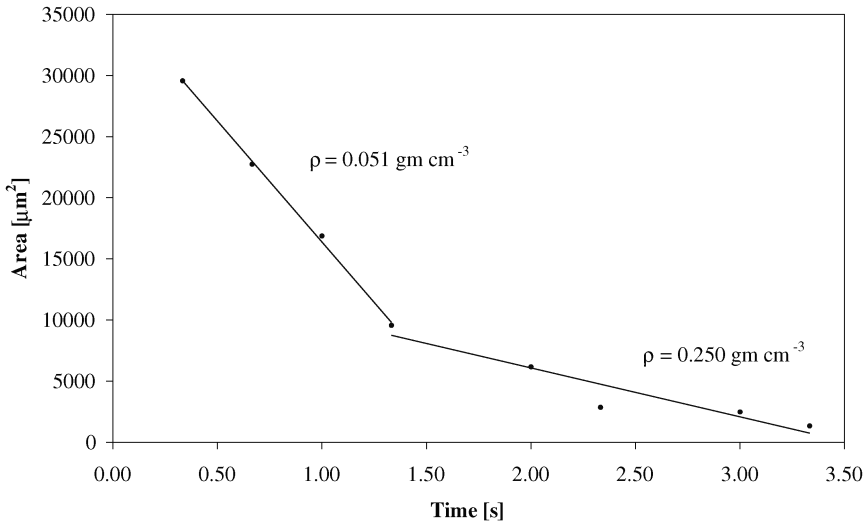

b)

Fig. 5 The evaporation rate (a) of an ice particle collected on the cloudscope window. The rate of area evaporation is linear (b) and inversely related to the particle density. The discontinuity in slope indicates a transition from a low-density exterior to a high-density center [17,19,23].

B. Energy Budget of Impacting Particles

A complete analysis of the energy budget of an impacting particle is complex and must assess the kinetic energy transferred to the surface energy during deformation and breakup. Surface and kinetic energy are also imparted to any departing particles resulting from splash or fracture. Table 1 shows the energy budget of drop impact and different conditions under which breakup ($L > 7$) is to be expected. The processes are quite different for an ice particle impact, as only particle fragmentation rather than deformation can occur. A drop may deform with increased surface and subsequently partly retract and partly wet the surface. During this process, some energy is converted to internal energy by viscosity and can be computed as a space and time integral of

$$\mu\left(\frac{\mathrm{d}u_i}{\mathrm{d}x_j}\right)^2 \tag{5}$$

over the motion of the drop, where μ is the dynamic viscosity of water, u and x are the velocity, and i, j, and k are the distance coordinates. As a crude initial approximation, this may be taken as $\mu(V/D)^2$, where V is the impact velocity and D is the drop diameter. In the case of an ice particle, things are different and yet more complex. The initial breakup takes place in milliseconds (0.00l s) as brittle fracture, requiring conversion of kinetic energy to ice surface energy (approximately 50% greater than water). Localization of the fracture depends on the details of the impact, as evident from the much smaller particles in some regions of Fig. 10 resulting from internal stress propagation [26]. Thus, an initial high-speed impact must result in crack propagation unrelated to crystallographic direction, as occurs in a localized impact on a glass sheet, whereas slower-speed impact leads to crack propagation along preferred crystallographic directions, parallel to the hexagonal faces and clearly shown in Fig. 10. Such effects were demonstrated by Gold [27], who initiated thermal stress by laying thin sheets of single

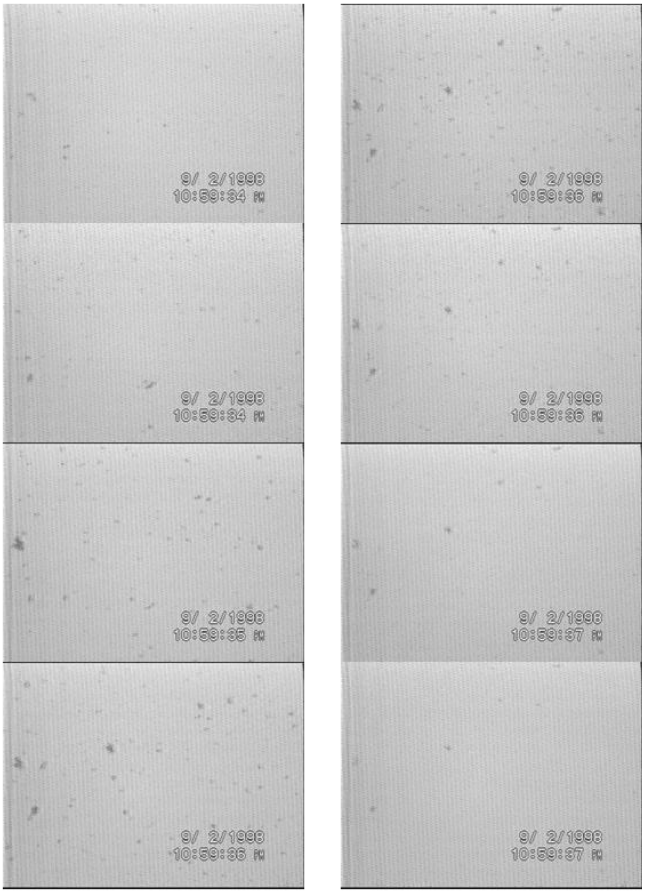

Fig. 6 Ice crystals accreting on the cloudscope at a surface temperature below 0°C and evaporating as individuals over a period of a few seconds. Air temperature: −30°C, stagnation temperature: −15°C, frame interval: about 1 s. Individual crystals can be tracked as they are collected and evaporate. Horizontal field of view is 1.5 cm.

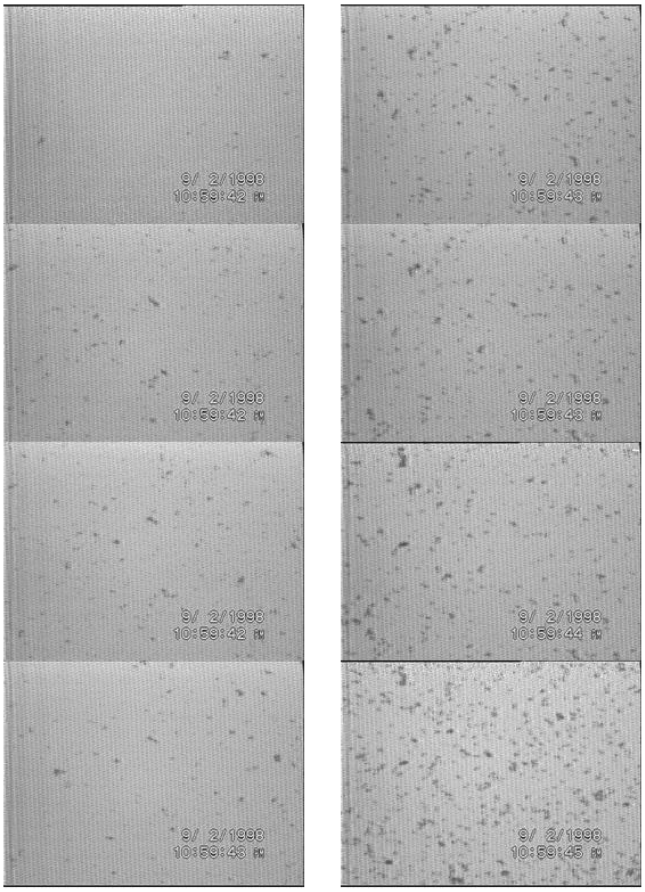

Fig. 7 As ice crystal size or concentration increases, impacting crystals overlap with partly evaporated crystals; some adhere but others are dislodged and removed into the airstream. Same conditions as Fig. 6.

crystalline ice on a metal surface some 40 deg colder. The final, slower part of the deformation (10 ms) may result from plastic deformation with the generation of internal dislocations in the ice also requiring energy [9,28].

Ice and water particles obviously behave differently, but similarities exist. The impact kinetic energy controls the initial behavior and relates to the impact velocity and particle mass. The Stokes number, *St*, is a measure of the stopping distance compared with the characteristic size of the impacting surface. The impacting velocity decreases as *St* becomes less than unity; small particles are not impacted at all, which is important for small cloud and aerosol-sized particles for aircraft conditions. The mass is estimated from particle geometry and an estimate of the density of the ice particles. For water, a spherical water drop suffices; for ice, the density, which may vary over the particle dimension, ranges from 0.05 to 0.92 having a complex geometry with air spaces. The surface energy ratio is computed from the initial geometry, deformed by a factor of 2 by an idealized spread and subsequently by a greater amount as a deformation to a thin disk. A splash occurs for a kinetic energy/initial surface energy ratio greater than about 7. For comparison, the energy involved in deformation is computed as a viscous loss under highly simplified assumptions of liquid shear (see notes in Table 1).

In the case of ice breakup, assumptions are made about the size of the shattered particles (as from Fig. 10) and the creation of surface energy, assuming uniform size as a first approximation at different thicknesses for the plate. Energy may also be deposited as defects within the ice lattice, but cannot be detected from the images. The geometry of the crystal breakup shown in Figs. 9–11 show localization of such fracture locations with the particle size approaching that of the optical resolution.

As shown in Figs. 14 and 16, ice particles are captured in a wetted surface produced by heating the surface and melting previously collected ice above 0°C. These particles rapidly melt, being swept aside in the divergent flow from the stagnation point. They may lodge at the outer melt boundary and build up there as an accretion under appropriate circumstances. All the observations discussed here are for near-normal impact; angled impact requires a separate study.

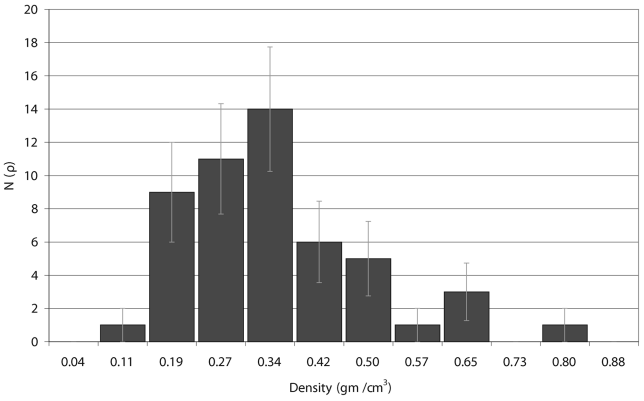

Fig. 8 Cloudscope measurements of the frequency of occurrence of ice particles of different density collected in the outflow from Hurricane Earl, 2 August 1998. Temperature: −45°C. A composite distribution of time segments from 10:59:51 to 11:00:00 [23].

IV. Conclusions

The general experience in the aviation community is that flight in glaciated clouds does not pose an icing risk to aircraft leading edges. It is shown here that this results from a balance of accretion and erosion. Ice *can* form on the stagnation point or lines but quickly reaches an equilibrium value of about 5 mm. Such an observation is

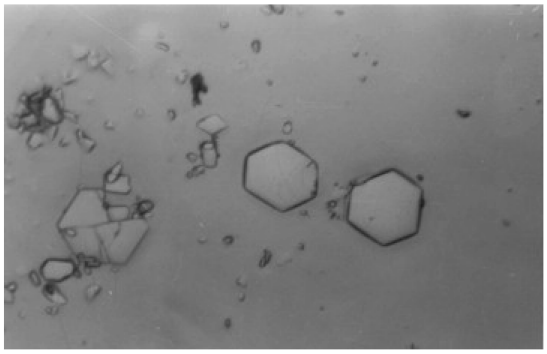

Fig. 9 Plates less than about 200 μm do not shatter on impact.

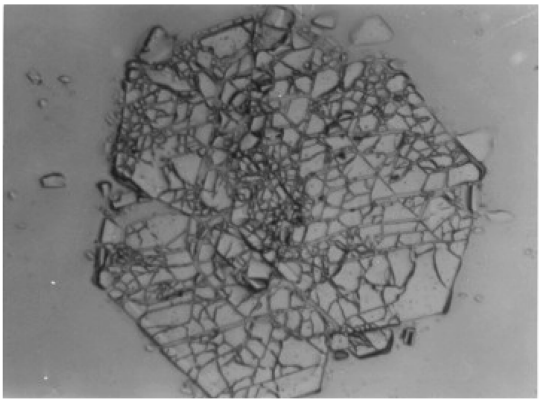

Fig. 10 A large ice plate collected in Formvar solution showing extensive shatter (in some cases parallel to the crystallographic axes). The size of the shattered fragments varies from place to place, suggesting a localization of stress following impact on collection.

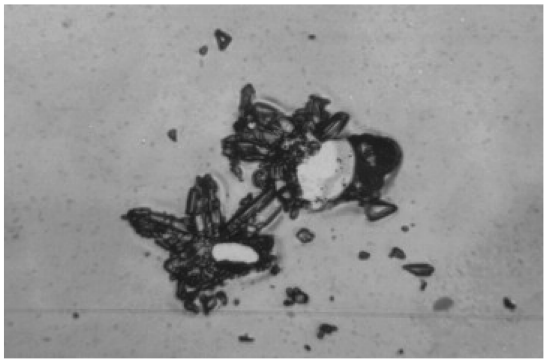

Fig. 11 A capped column shows complex fracture behavior on collection.

demonstrated and consistent with the measurements made with the cloudscope. Table A1 summarizes the range of particle characteristics and their possible interactions with aircraft surfaces.

For determining the effects on an aircraft with a failed leading-edge de-icing system, ice shapes are actually physically installed on the aircraft and the resulting lack of lift is documented through in-flight tests. The same type of test can be done using computer simulations. The actual ice shapes used are usually produced through computer simulations, which are verified using all-liquid wind-tunnel experiments or some in-flight measurements. For mixed-phase clouds, it is intuitive that the ice shapes that would form would be different than those in an all-liquid cloud. Impacting ice particles could potentially lead to rougher surfaces or even erode some portions of the surface. It is yet to be determined whether these different shapes would be more or less hazardous.

For thermally de-iced surfaces, the observations from the cloudscope suggest that the bulk of the accreted ice appears to melt quickly; then the system must shed the resulting liquid, either

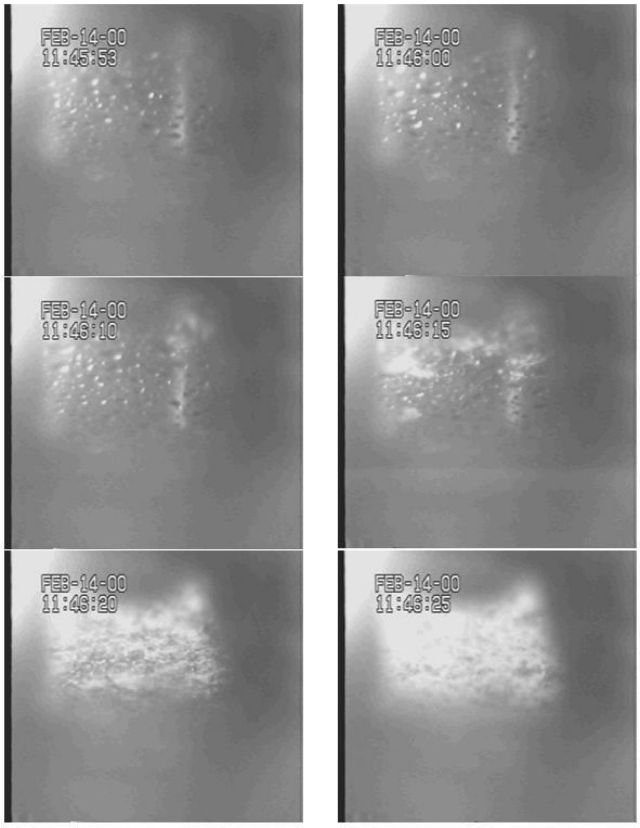

Fig. 12 A sideways slightly angled view of particles collected on the large format cloudscope showing a sequence as the window is cooled over a 32 s interval. Data were collected at 1/90 s to show collection detail. The size of illuminated part 1 cm. At surface temperatures above freezing, ice particles quickly melt on accretion. As the heating is reduced to a surface temperature of colder than 0°C, ice particles quickly accrete and build up. Sideways viewing leads to an estimate of particle volume. The ambient conditions were as follows: static temperature, −8.8°C; altitude, 11 kft; Nevzorov liquid-water content, 0.02 g m^{-3}; total water content, 0.124 g m^{-3}. The view comes through the prism shown in Fig. 2 at the bottom of the window. The region goes out of focus at the edges.

through evaporation or runoff. The cloudscope measurements concentrate on impactions near the stagnation point, but it is expected that some fraction of the ice will also adhere and melt at distances well beyond the stagnation point. That fraction needs to be determined with future in-flight work with a modified cloudscope or with wind-tunnel simulations with ice particles having realistic properties.

It should be mentioned that pilots can report seeing "rain" on a heated windscreen when flying at very cold temperatures. Cloudscope measurements (e.g., Fig. 12) clearly show that ice crystals impacting a heated surface melt very quickly and give the appearance of encountering liquid drops. Pilots should be made aware of this phenomenon.

Do ice particles bounce when they hit the stagnation point or at some distances beyond the stagnation point? The cloudscope measurements show that a considerable fraction of the particles stick to the surface without bouncing. Anyone who drives an automobile during the winter also experiences snowflakes hitting the warm windshield, sticking, and melting. Again, to quantify the "sticking coefficient," it would be necessary to do more work. It is anticipated that the sticking coefficient would increase when liquid drops are also present or when the surface is heated, hypotheses requiring testing.

These considerations suggest that wind-tunnel simulation of the icing process in a mixed cloud must take into account the scale of ice and supercooled water as it interacts with the target. As discussed earlier, a mixed-phase cloud can be considered homogeneously or heterogeneously mixed, the latter a cloud with a varying scale of all ice to all water following the wind flow. Simulating these conditions

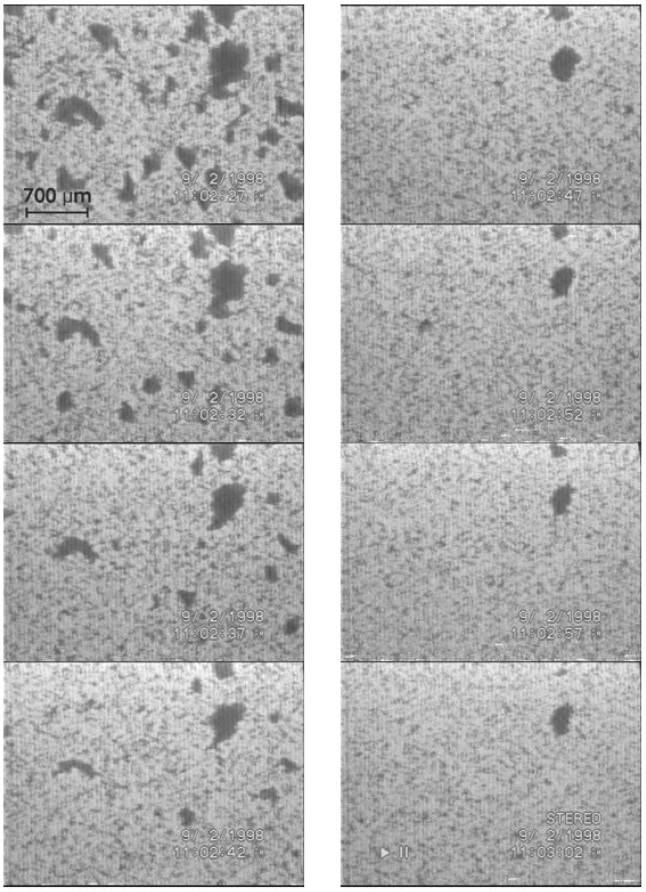

Fig. 13 Accretion of larger ice particles (500 μm) followed by much smaller ice particles (50 μm) leads to spectacular erosion of the larger particles as pieces irregularly disappear from the field of view. The larger (apparently black) pieces collected earlier have nearly completely eroded after a few seconds. Field of view is 1.5 cm.

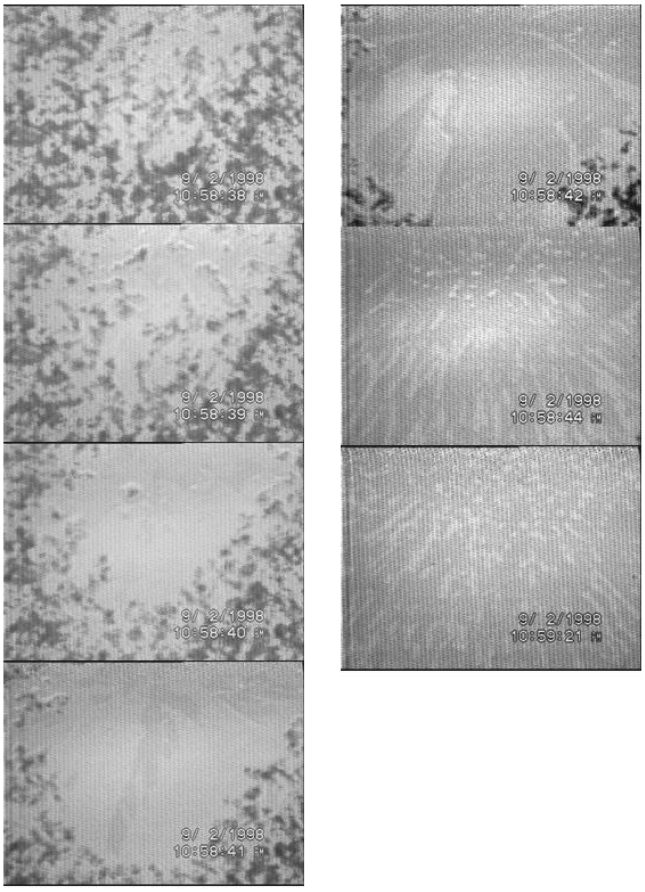

Fig. 14 Ice particles collected at near −30°C heated to melting. The stagnation point is top center of each image, most clearly shown by the flow streaks in the three right-hand images. The melting particles are carried outward by the airflow away from the stagnation point (3,4); incoming ice particles quickly (a few frames of 1/30 s) melt on impacting the region of >0°C, and their remnants are similarly carried outward as droplets (last 3 of sequence). Field of view is 1.5 cm.

is a major technological challenge; not only is the situation highly transient, as the crystals grow and fall out, but the crystals themselves are to be specified by habit and size. This could only be achieved by uniform nucleation (as by the pressure differential in the spray nozzles) and growth in a large thermal moisture diffusion chamber throughout a given cross section at a specified temperature and time ahead of the test section with the fraction of ice to water controlled by input and the mixing of two nearly parallel airstreams. After all cloud evaporated, a continuous inflow of vapor-grown crystals of uniform size and habit would be achieved in the complete absence of supercooled water. On a small scale, plenty of supercooled cloud and ice crystals of uniform size/habit may be alternated at selected times through the test section or by parallel flow regions of water and ice to investigate the changing accretion.

A considerable effort has been expended on studying supercooled large drops (with diameters of >50 μm) because they can impact beyond the normally protected airfoil surfaces and subsequently freeze. Bouncing and splashing are also a concern in quantifying such accretions. For ice crystals in mixed or glaciated clouds, a similar problem exists. The larger ice particles can impact further back on the airfoil. For a running wet thermal system, if an ice crystal impacts on a liquid layer, the chances of sticking probably increase. A supercooled water layer runback may be subject to nucleation. For such a wet thermal system, there also exists a potential problem in which the runback can consist of an ice/liquid mixture.

Because mixed-phase clouds occur quite frequently [2,6,7] with total water contents very similar to all-liquid clouds, it would seem prudent to study the accretion of water (both liquid and solid) on aircraft surfaces in more detail. At least for thermally de-iced systems, it would also seem prudent to design such systems using total water content (liquid plus solid) for the design criteria, instead of liquid-water content alone.

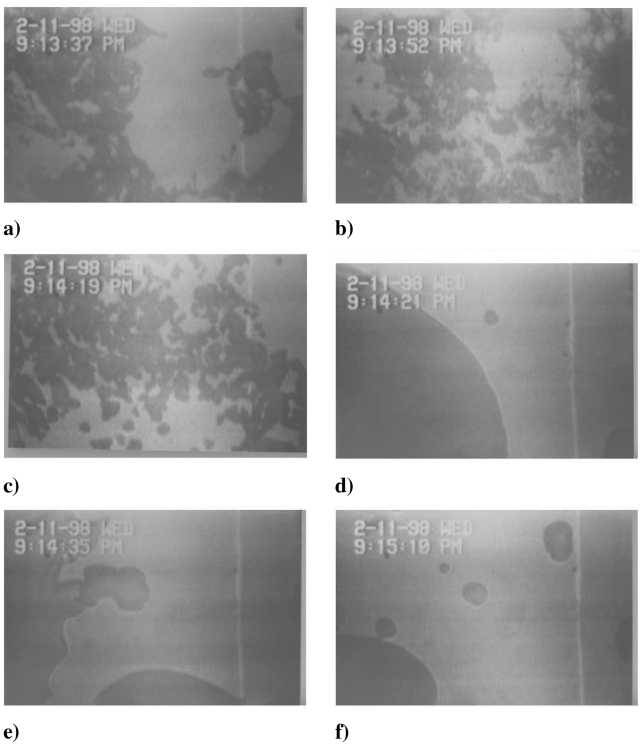

Fig. 15 As Fig. 14, only collected by the higher-resolution cloudscope (horizontal field of view 1/2 mm). a), b), and c) ice accretion; d), e), and f) supercooled water drops collected simultaneously.

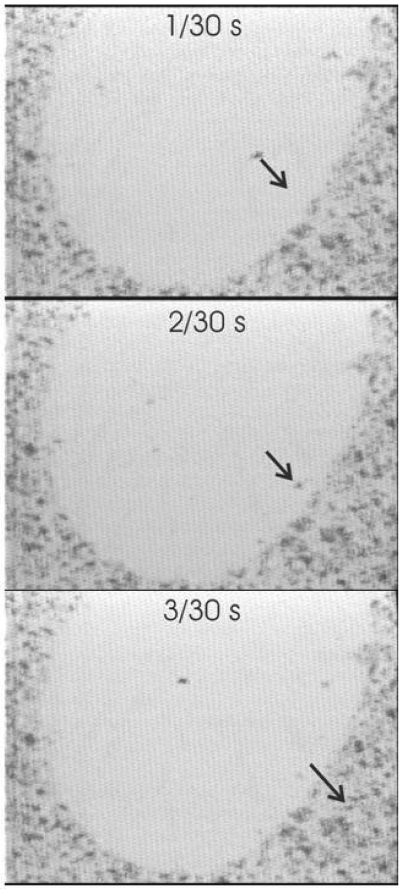

Fig. 16 A sequence showing a crystal impacting, sliding toward the edge in the second frame, and then sliding into the periphery, possibly after colliding with a new particle. Sequence follows Fig. 14.

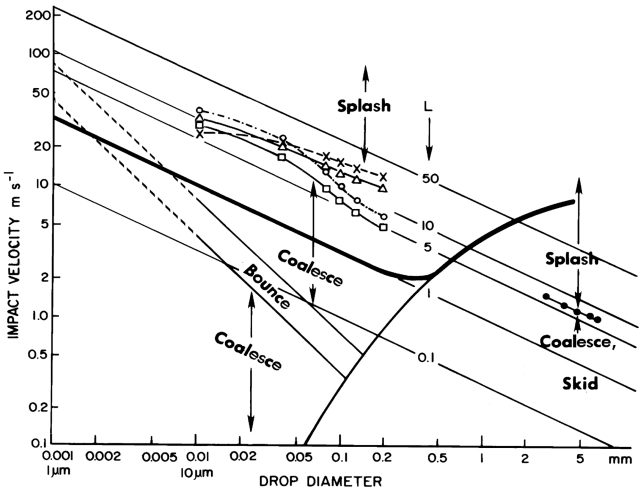

Fig. 17 Criteria for water drop break up on impaction in terms of the initial kinetic energy/surface energy ratio, *L*, for the range of 50–0.1. For entry into a water surface at terminal velocity in air at 0°C and 1 atm pressure, the thick line (total energy, surface plus kinetic) shows a diameter greater than about $\frac{1}{2}$ mm dominated by fall velocity with a splash criterion, *L*, between 7 and 20. Smaller drops, with surface energy dominating, coalesce and propagate into the liquid as a vortex ring with an equivalent velocity. At a higher impact velocity, the splash behavior on a solid surface is further influenced by material and surface roughness (full circles: deep water; open circles: clear, wet ice; crosses: wax). In the case of an ice layer covered with a finite liquid layer, the drop propagates as a vortex ring and carries supercooled liquid directly to the ice surface, leading to its growth [25].

The FAA 1998 Workshop [5] concluded "the workshop did not indicate that structural ice in mixed-phase conditions posed special performance problems for aircraft. However, the relevant data are very limited." It was further concluded that it would require a large investment to further advance our knowledge in this area. This paper demonstrates that progress can be made with modest efforts. Because the problem is potentially quite significant, further work should be performed.

Table 1 Energy budget of a drop impact, deformation, and splash (energy in joules). A velocity *V* of 100 and 150 m/s represents impact at aircraft speed. Splash also occurs with particles falling at terminal velocity, providing *L* is greater than 7 and kinetic energy, in column 3, is greater than viscous loss, in columns 6 and 7

Drop diameter D, μm	Velocity V Terminal V_T, m/s[a]	Kinetic energy (KE) at velocity V[b]	Surface energy (SE)[c]	L = KE/SE (Splash>7)[d]	Viscous loss[e]	
	——	$0.25D^3V^2 \times 10^{-7}$	$250D^2 \times 10^{-7}$	$DV^2/1000$	Surface area doubles $0.0005VD^2$	Drop deforms to disk diameter $10D$ $0.002VD^2$
10	$V_T = 0.003$	2.5×10^{-18}	2.5×10^{-11}	1×10^{-7}	1.5×10^{-16}	6×10^{-15}
	1	2.5×10^{-13}		1×10^{-2}	5×10^{-14}	2×10^{-12}
	10	2.5×10^{-11}		1.0	5×10^{-13}	2×10^{-11}
	100	2.5×10^{-9}		**100**	5×10^{-12}	2×10^{-10}
	150	5.6×10^{-9}		**225**	7.5×10^{-12}	3×10^{-10}
100	$V_T = 0.3$	2×10^{-11}	2.5×10^{-9}	0.009	1.5×10^{-12}	6×10^{-11}
	1	2.5×10^{-10}		0.1	5×10^{-12}	2×10^{-10}
	10	2.5×10^{-8}		**10**	5×10^{-11}	2×10^{-9}
	100	2.5×10^{-6}		**1000**	5×10^{-10}	2×10^{-8}
	150	5.6×10^{-6}		**2250**	7.5×10^{-10}	3×10^{-8}
1000	$V_T = 5$	62.5×10^{-7}	2.5×10^{-7}	**25**	2.5×10^{-9}	1.0×10^{-7}
	1	2.5×10^{-7}		1	5×10^{-10}	0.2×10^{-7}
	10	2.5×10^{-5}		**1×10^2**	5×10^{-9}	2×10^{-7}
	100	2.5×10^{-3}		**1×10^4**	0.5×10^{-7}	20×10^{-7}
	150	5.6×10^{-3}		**2.25×10^4**	0.75×10^{-7}	30×10^{-7}

[a] V_T: Standard atmosphere, −8°C.
[b] Kinetic Energy: D is the particle diameter, V is the impact velocity, V_T is the terminal velocity, 1, 10, 100, 150 m/s, $0.25D^3V^2$.
[c] Surface energy area X surface energy 0.079 J/m^2 water at −8°C. Drops assumed initially spherical, deformed to twice the sphere area or deformed to a uniform disk diameter of 10 × drop diameter with the mass conserved neglecting the edge energy.
[d] Kinetic energy/surface energy for a spherical drop: $DV^2/1000$ [25], giving empirical evidence for splash of drops for a kinetic energy/surface energy ratio of greater than 7.
[e] Viscous loss computed from Eq. (1) assuming a sphere diameter of D with an impact velocity difference across its radius, as a drop under low gravity or in the midstage of oscillation, compared with a deformed drop, falling at terminal velocity in air having approximately double the surface area. This is compared with a drop impacting on a flat surface at terminal velocity and at 1, 10, 100, and 150 m/s, deforming to a thin disk diameter of $10D$, splashing by breakup at the periphery at the higher velocities, having approximately $x10$ of the surface area. The viscosity energy losses (joules) are calculated for a spherical drop deformed on impact to a hemisphere (giving a shear and a time for deformation). Taking water dynamic viscosity μ at 20°C 0.001 Pa · s gives energy loss as $0.0005VD^2$ (column 6). For a drop deformed to a $10D$ disk, the time is comparable but the shear greater, $0.002VD^2$ (column 7).

Appendix: Particle Characteristics

Table A1 Temperature-dependent particle characteristics[a]

Temperature	Process				
		Primary particles[b]		Aircraft interaction[c]	Surface condition
−50 °C		Rosette aggregation			
		Survival of supersaturated solution drops before dilution	Evaporating ice breakup		
−40 °C		All supercooled water drops frozen; no rime	Evaporating ice breakup	Collapse and erosion on impact	Initial frozen fraction
−30 °C	Supercooled drop coalescence			Minimal ice aggregation	
					$\Delta T/L_f$[d]
−20 °C	Supercooled drop coalescence			Impacted water drops collected or splash[e]	
		Rime; supercooled drops impact and freeze as sphere segment	Evaporating ice breakup	Crystals impact [9,28], break up, and erode	
				Supercooled drop collection though a liquid layer overlying an ice substrate	Supercooled drop accretion likely
−15 °C		Dendrite			Mixed accretion [d] more likely at temperatures between −15 and −35 °C
		Crystal aggregation			
−10 °C	Supercooled drop coalescence and break up				
		Rime: drops spread more and freeze; ice accretion and bounce	Liquid layers for wet growth; splash and skid increasing with impact velocity	Impacted water drops collected or splash	Dry growth more likely at low velocity and low liquid-water content
		Crystal collected by supercooled drop			
−5°C		Column crystal aggregation	Liquid layers for wet growth; splash and skid increasing with impact velocity	Impacted water drops collected or splash	Wet growth more likely for higher velocity impact and higher liquid-water content;
				Supercooled drop accretion likely	
0°C		Ice accretion		Mixed accretion less likely	Decreasing frozen fraction with increasing temperature for individual drops
0°C			Temperatures may be ice bulb, wet bulb, melting/freezing		
	Drop coalescence and break up		Melting snow; decreasing ice fraction at lower levels	Impacted mix collected or splashed	
+5°C		Melting crystals collected by drops; partly melted snow sheds drops	Falling crystals melt and break up	Impacted water drops collected or splashed	
			Liquid layers form drops on columns and dendrites		
			Falling graupel and hail melts; water shed[f]		
+10°C				Impacted water drops collected or splash	
+20°C	Drop coalescence and breakup				

[a]The impact of particles on aircraft surfaces and accreted ice below 0°C are comparable except when the ice is covered with a liquid layer during melt or when impact rates are sufficient for latent heat water–ice transition to raise the temperature to near 0°C. The surface of the water layer can be supercooled away from the ice interface following the impaction and coalescence of supercooled cloud drops.

[b]Ice crystals growing from a vapor have highly complex shapes and densities; some forms of ice growth from the vapor are similar to ice accretion but some are not [29].

[c]Aircraft collection of supercooled water occurs under comparable conditions to large (10-cm-diam) hail with a fall velocity of 50 m/s, which determines air bubble and ice crystal structure.

[d]Supercooled drops after nucleation are a mix of dendrites and water, with the fraction dependent on supercooling by the ratio of supercooling to latent heat, $\frac{\Delta T}{L_f}$, and maintain a temperature close to 0°C until completely frozen. Impact during this freezing period leads to a slushy snowball-type breakup [30,31].

[e]The drop splash [25] is the same at below or above 0°C except when freezing has been initiated as impact cavitation.

[f]Partly melted snow flakes have drops distributed over crystal intersections and along individual columns or dendrites [32,33].

Acknowledgments

The authors would like to acknowledge the Federal Aviation Administration through the Meteorological Service of Canada, KM175-1-2150; the National Science Foundation, ATM9900560; the U.S. Air Force (cloudscope design and construction), F49620-00-1-0215; NASA, NAG-1 1046; and the Tropical Rainfall Measuring Mission, NAG5-9716. The Canadian National Search and Rescue Secretariat, Transport Canada, and the National Research Council (NRC) also supported this research.

References

[1] Federal Aviation Administration, "U. S. Code of Federal Regulations," Title 14 (Aeronautics and Space), Part 25 (Airworthiness Standard: Transport Category Airplanes), Appendix C, National Archives and Records Administration, U.S. Government Printing Office, Washington D. C., 1999

[2] Cober, S. G., and Isaac, G. A., "Aircraft Icing Environments Observed in Mixed Phase Clouds," AIAA Paper 2002-0675, Jan. 2002.

[3] "In-Flight Icing Encounter and Loss of Control Simmons Airlines," d.b.a. American Eagle Flight 4184, Avions de Transport Regional (ATR) Mdel 72-212, N401AM Roselawn, Indiana, National Transportation Safety Board Safety Board Report. PB96-91040, NTSB/AAR-96-O1, DCA95MA001, Vol. 1, 1996.

[4] "In-Flight Icing Encounter and Uncontrolled Collision with Terrain," Comair Flight 3272, Embraer EMB-120RT, N265CA, Monroe, Michigan, National Transportation Safety Board, Rept. PB98-910404'l, NTSB/AAR-98/04, DCA97/MA017, 1998.

[5] Riley, J. T., "Mixed Phase Icing Conditions: A Review," Office of Aviation Research DOT/FAA/AR-98/76, Dec. 1998.

[6] Cober, S. G., Isaac, G. A., Korolev, A. V., and Strapp, J. W., "Assessing Cloud-Phase Conditions," *Journal of Applied Meteorology*, Vol. 40, No. 11, Nov. 2001, pp. 1967–1983. doi:10.1175/1520-0450(2001)040<1967:ACPC>2.0.CO;2

[7] Korolev, A. V., Isaac, G. A., Cober, S. G., Strapp, J. W., and Hallett, J., "Observations of the Microstructure of Mixed Phase Clouds," *Quarterly Journal of the Royal Meteorological Society*, Vol. 129, No. 587, 2003, pp. 39–65. doi:10.1256/qj.01.204

[8] Hallett, J., Purcell, R., Roberts, M., Vidaurre, G., and Wermers, D., "Measurement for Characterization of Mixed Phase Clouds," AIAA Paper 862, Jan. 2005.

[9] Vidaurre, G., and Hallett, J., "Particle Impact and Breakup in Aircraft Measurement," *Journal of Atmospheric and Oceanic Technology* (submitted for publication).

[10] Hallett, J., "Charge Generation with and Without Secondary Ice Production," *11th International Conference on Atmospheric Electricity*,CP 209261, NASA, Washington, D. C., June 1999, pp. 355–358.

[11] Hallett, J., and Vidaurre, G., "High Resolution Measurement of Ice–Supercooled Water Cloud Interfaces," American Meteorological Society Paper 3.3, July 2006.

[12] Isaac, G. A., Cober, S. G., Strapp, J. W., Korolev, A. V., Tremblay, A., and Marcotte, D. L., "Recent Canadian Research on Aircraft In-Flight Icing," *Canadian Aeronautics and Space Journal*, Vol. 47, No. 3, Sept. 2001, pp. 213–221.

[13] Isaac, G. A., Ayers, J. K., Bailey, M., Bissonnette, L., Bernstein, B. C., Cober, S. C., Driedger, N., Evans, W. F. J., Fabry, F., Glazer, A., Gultepe, I., Hallett, J., Hudak, D., Korolev, A. V., Marcotte, D., Minnis, P., Murray, J., Nguyen, L., Ratvasky, T. P., Reehorst, A., Reid, J., Rodriguez, P., Schneider, T., Sheppard, B. E., Strapp, J. W., and Wolde, M., "First Results from the Alliance Icing Research Study II," AIAA Paper 2005-0252, Jan. 2005.

[14] Knollenberg, R. G., "Techniques for Probing Cloud Microstructure," *Clouds, Their Formation, Optical Properties, and Effects*, edited by P. V. Hobbs, and A. Deepak, Academic Press, New York/London/Orlando, FL, 1981.

[15] Lawson, R. P., Baker, B. A., and Schmitt, C. G., "An Overview of Microphysical Properties of Arctic Clouds Observed in May and July 1998 During FIRE ACE," *Journal of Geophysical Research*, Vol. 106, No. D14, 2001, pp. 14989-15014. doi:10.1029/2000JD900789

[16] Arnott, W. P., Dong, Y., Purcell, R., and Hallett, J., "Direct Airborne Sampling of Small Ice Crystals and the Concentration and Phase of Haze Particles," *9th Symposium on Meteorological Observations and Instrumentation*, American Meteorological Society, Boston, MA, 1995, pp. 415–420; also American Meteorological Society Paper 11.2.

[17] Hallett, J., Arnott, W. P., Purcell, R., and Schmidt, C., "A Technique for Characterizing Aerosol and Cloud Particles by Real Time Processing, PM2.5: A Fine Particle Standard," *Proceedings of the International Specialty Conference, Sponsored by EPA, Air & Waste Management Association*, edited by J. Chow and P. Koutrakis, Vol. 1, Air & Waste Management Association, Pittsburgh PA, 1998, pp. 318–325.

[18] Meyers, M. B., and Hallett, J., "Micrometer-Sized Hygroscopic Particles in the Atmosphere: Aircraft Measurement in the Artic," *Journal of Geophysical Research*, Vol. 106, No. D24, 2001, pp. 34067-34080. doi:10.1029/2001JD000652

[19] Garner, B., "On the Density of Ice Particles," Master's Thesis, University of Nevada, Reno, NV, 2001.

[20] MacCready, P., and Todd, C., "Continuous Particle Sampler," *Journal of Applied Meteorology*, Vol. 3, No. 4, Aug. 1964, pp. 450–460. doi:10.1175/1520-0450(1964)003<0450:CPS>2.0.CO;2

[21] Hallett, J., "Measurement of Size, Concentration and Structure of Atmospheric Particulates by the Airborne Continuous Particle Replicator," Air Force Geophysics Laboratory, Hanscom Air Force Base, AFGL-TR 76-0149, 1976.

[22] Middleman, S., *Modeling Axi-Symmetric Flows*, Academic Press, New York/London/Orlando, FL, 1995.

[23] Garner, B., and Hallett, J., "On the Density of Atmospheric Ice Particles in Tropical Convection," *Journal of the Atmospheric Sciences* (submitted for publication).

[24] Korolev, A. V., Bailey, M. P., Hallett, J., and Isaac, G., "Laboratory and In Situ Observation of Deposition Growth of Frozen Drops," *Journal of Applied Meteorology*, Vol. 43, No. 4, 2004, pp. 612–622. doi:10.1175/1520-0450(2004)043<0612:LAISOO>2.0.CO;2

[25] Hallett, J., and Christensen, L., "The Splashing and Penetration of Raindrops into Water," *Journal de Recherches Atmosphériques*, Vol. 18, No. 4, Oct.–Dec. 1984, pp. 226–242.

[26] Renshaw, C. E., and Schulson, E. M., "Universal Behaviour in Compressive Failure of Brittle Materials," *Nature (London)*, Vol. 412, Aug. 2001, pp. 897–900. doi:10.1038/35091045

[27] Gold, L., "Formation of Cracks in Ice Plates by Thermal Shock," *Nature*, Vol. 192, Oct. 1961, pp. 130–131. doi:10.1038/192130a0

[28] Vidaurre, G., and Hallett, J., "Energetics of Mixed Phase Cloud Particle Interactions," American Meteorological Society Paper P2.54, July 2006.

[29] Bailey, M., and Hallett, J., "Growth Rates and Habits of Ice Crystals Between −20°C and −70°C," *Journal of the Atmospheric Sciences*, Vol. 61, No. 5, March 2004, pp. 514–544. doi:10.1175/1520-0469(2004)061<0514:GRAHOI>2.0.CO;2

[30] Johnson, D., and Hallett, J., "Freezing and Shattering of Supercooled Water Drops," *Quarterly Journal of the Royal Meteorological Society*, Vol. 94, No. 402, 1968, pp. 468–482. doi:10.1002/qj.49709440204

[31] Black, R. A., Heymsfield, G. M., and Hallett, J., "Extra Large Particle Images at 12 km in a Hurricane Eyewall: Evidence of High-Altitude Supercooled Water?," *Geophysical Research Letters*, Vol. 30, No. 21, 2003, pp. 10-1–10-4. doi:10.1029/2003GL017864.

[32] Oraltay, R. G., and Hallett, J., "The Melting Layer: A Laboratory Investigation of Ice Particle Melt and Evaporation Near 0°C," *Journal of Applied Meteorology*, Vol. 44, No. 2, Feb. 2005, pp. 206–220. doi:10.1175/JAM2194.1

[33] Knight, C., "Observations of the Morphology of Melting Snow," *Journal of the Atmospheric Sciences*, Vol. 36, No. 6, June 1979, pp. 1123–1130.